

Defect Solitons in Parity-Time Symmetric Optical Lattices with Nonlocal Nonlinearity

Sumei Hu,^{1,2} Xuekai Ma,¹ Daquan Lu,¹ Yizhou Zheng,¹ and Wei Hu^{1,*}

¹Laboratory of Nanophotonic Functional Materials and Devices,
South China Normal University, Guangzhou 510631, P. R. China

²Department of physics, Guangdong University of Petrochemical Technology, Maoming 525000, P. R. China

The existence and stability of defect solitons in parity-time (PT) symmetric optical lattices with nonlocal nonlinearity are reported. It is found that nonlocality can expand the stability region of defect solitons. For positive or zero defects, fundamental and dipole solitons can exist stably in the semi-infinite gap and the first gap, respectively. For negative defects, fundamental solitons can be stable in both the semi-infinite gap and the first gap, whereas dipole solitons are unstable in the first gap. There exist a maximum degree of nonlocal nonlinearity, above which the fundamental solitons in the semi-infinite gap and the dipole solitons in the first gap do not exist for negative defects. The influence of the imaginary part of the PT-symmetric potentials on soliton stability is given. When the modulation depth of the PT-symmetric lattices is small, defect solitons can be stable for positive and zero defects, even if the PT-symmetric potential is above the phase transition point.

PACS numbers: 42.25.Bs, 42.65.Tg, 11.30.Er

I. INTRODUCTION

The physical systems with parity-time (PT) symmetry have attracted much more attention in recent years [1–10]. Bender *et al.* found that PT-symmetric Hamiltonians can have entirely real spectra although these Hamiltonians are non-Hermitian [1, 2]. In optics, PT-symmetric structures can be constructed by inclusion of gain or loss regions into waveguides, which make the complex refractive-index distribution obeying the condition $n(x) = n^*(-x)$ [3–5]. Many unusual features stemming from the PT-symmetry have been found, such as power oscillation [5, 10, 11], absorption enhanced transmission [9], nonlinear switching structure [12, 13], and unidirectional invisibility [14]. In experiments, the PT-symmetry breaking in complex optical potentials was observed firstly by Guo *et al.* in a double-well structure fabricated through a multilayer $Al_xGa_{1-x}As$ heterostructure with varying concentrations [9]. Rüter *et al.* observed the non-reciprocal wave propagation in an active PT-symmetric coupled waveguide system based on Fe-doped $LiNbO_3$, in which optical gain is provided through two-wave mixing using the photorefractive nonlinearity [10]. Those theoretical and experimental results led to the proposal of a new class of PT-symmetric synthetic materials with intriguing and unexpected properties that rely on the non-reciprocal light propagation [10, 14].

In optics, nonlinearities in the PT-symmetric systems have been considered by many authors [8, 13–16], especially in the PT-symmetric optical lattices [4, 5, 14], and some new kinds of soliton were found and investigated [4, 17–20]. Defect solitons can be formed when a local defect is introduced into the optical lattices, which have been widely studied in the regimes of photonic crystals, waveguide arrays, and optically induced photonic lattices

[21–23]. Due to its unique properties based on the defect guiding phenomena which can be controlled through variation of the defect parameters [24], defect solitons have the potential applications for the all-optical switches and routing of optical signals [25]. Zhou *et al.* have studied the defect modes in the PT-symmetric optical lattices [18]. Defect solitons in PT-symmetric optical lattices and superlattices with local nonlinearity have been studied, and stable solitons are found mainly in the semi-infinite gap [19, 20].

It is noteworthy that the nonlinearity in the photorefractive media, in which Rüter *et al.* have observed the non-reciprocal wave propagation [10], is nonlocal due to the diffusion mechanism of charge carriers [26–28]. The nonlocality of nonlinear response exists in many real physical systems, such as photorefractive crystals [26–28], nematic liquid crystals [29–31], lead glasses [32, 33], etc. The nonlocality can drastically modify the properties of solitons and improve the stability of solitons [34–36]. Therefore it is worthy to study the properties of solitons in PT-symmetric optical lattices with nonlocal nonlinearity.

In this paper, we study defect solitons in PT-symmetric optical lattices with nonlocal nonlinearity. The properties of nonlocal defect solitons are quite different from those in local media, and the nonlocality can expand the stability regions of soliton, especially in the first gap. It is found that the stability of nonlocal defect solitons depends on the defect, the degree of nonlocality, and the PT-symmetric potentials. The influence of the imaginary part of the PT-symmetric potentials is studied, and the example of stable soliton in the PT-symmetric potentials above the phase transition point is given.

* Corresponding author's email address: huwei@scnu.edu.cn

II. THEORETICAL MODEL

We consider the propagation of light beam in the PT-symmetric defective lattices with Kerr-type nonlocal nonlinearity. The evolution of complex amplitude U of the light fields can be described by following dimensionless nonlinear Schrödinger equation (NLSE),

$$i\frac{\partial U}{\partial z} + \frac{1}{2}\frac{\partial^2 U}{\partial x^2} + p[V(x) + iW(x)]U + nU = 0, \quad (1)$$

where x and z are the transverse and longitudinal coordinates, respectively, and p is the depth of the PT-symmetric potentials. $V(x)$ and $W(x)$ are the real and imaginary parts of the PT-symmetric potentials, respectively, which are assumed in this paper as

$$V(x) = \cos^2(x)[1 + \epsilon \exp(-x^8/128)], \quad (2)$$

$$W(x) = W_0 \sin(2x). \quad (3)$$

Here ϵ represents the strength of the defect, which is expressed as a super-Gaussian profile [19]. The parameter W_0 represents the strength of the imaginary part of the PT-symmetric potentials compared with the real part.

The nonlinear refractive-index change n satisfies

$$n - d\frac{\partial^2 n}{\partial x^2} = |U|^2, \quad (4)$$

where d stands for the nonlocality degree of the nonlinear response. This type of nonlinear response with a finite region of nonlocality exists in many real physical systems, for instance, all diffusion-type nonlinearity [28, 37, 38], orientational-type nonlinearity [31, 39], and the general quadratic nonlinearity describing parametric interaction [40, 41]. Although the diffusion nonlinearity in photorefractive media is anisotropic, Eq. (4) can still be used to describe its nonlocal feature theoretically when we ignore the anisotropic effect [42]. Moreover when $d \rightarrow 0$, the above equation reduces to $n = |U|^2$, and Eq. (1) reduces to that for local case. When $d \neq 0$, Eqs. (1) and (4) denote a nonlocal NLSE with an exponential-decay type nonlocal response.

The PT-symmetric lattices governed by Eq. (2) have Bloch band structures when $\epsilon = 0$. The band diagram can be entirely real when the system is operated below the phase transition point ($W_0^c = 0.5$) [4, 5]. The Bloch band structure obtained by the plane wave expansion method for $p = 4$ is shown in Fig.1(a). From Fig. 1(a), we can see that the region of the first gap decreases with increasing W_0 . The first gap disappears when $W_0 = 0.5$, which is the phase transition point. When the system is above the phase transition point, i.e. $W_0 > 0.5$, the band structure becomes complex. Figures 1(b)-1(d) show the profiles of the PT-symmetric potentials for $p = 4$ and $W_0 = 0.1$ with positive defects ($\epsilon = 0.5$), zero defects ($\epsilon = 0$), and negative defects ($\epsilon = -0.5$), respectively.

We search for stationary solutions to Eqs. (1) and (4) in the form $U = f(x)\exp(ibz)$, where $f(x)$ is a complex

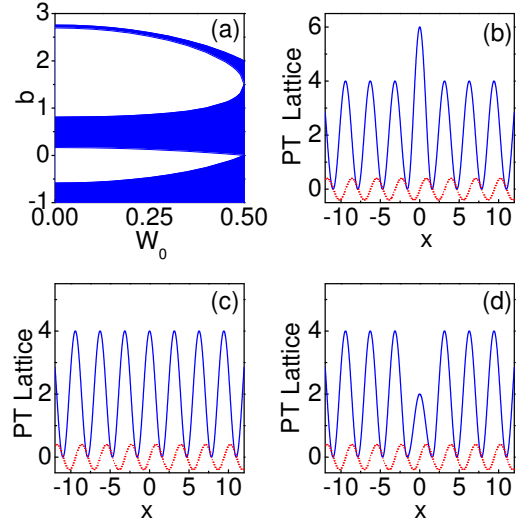


FIG. 1. (color online) (a) Band structure for the PT-symmetric lattice with $p = 4$; The blue regions are bands while the blank regions are gaps. (b)-(d) Lattice profiles for lattices with $p = 4$, $W_0 = 0.1$, and (b) $\epsilon = 0.5$, (c) $\epsilon = 0$, and (d) $\epsilon = -0.5$, respectively. Solid blue and dotted red lines represent the real and imaginary parts, respectively.

function satisfies equations,

$$bf = \frac{1}{2}\frac{\partial^2 f}{\partial x^2} + p[V(x) + iW(x)]f + nf, \quad (5)$$

$$n - d\frac{\partial^2 n}{\partial x^2} = |f|^2. \quad (6)$$

The solutions of defect solitons are gotten numerically by the modified squared-operator method [43] from Eqs. (5) and (6) and shown in the next section. To elucidate the stability of defect solitons, we search for perturbed solution to Eqs. (1) and (4) in the form $U(x, z) = [f(x) + u(x, z) + iv(x, z)]\exp(ibz)$, where the real $[u(x, z)]$ and imaginary $[v(x, z)]$ parts of the perturbation can grow with a complex rate δ upon propagation. Linearization of Eq. (1) around the stationary solution $f(x)$ yields the eigenvalue problem,

$$\begin{aligned} \delta v = & \frac{1}{2}\frac{\partial^2 u}{\partial x^2} + (n - b)u + p(Vu - Wv) \\ & + \text{Re}[f(x)] \int_{-\infty}^{\infty} 2G(x - \xi)u(\xi)\text{Re}[f(\xi)]d\xi \\ & + \text{Re}[f(x)] \int_{-\infty}^{\infty} 2G(x - \xi)\text{Im}[f(\xi)]v(\xi)d\xi, \end{aligned} \quad (7)$$

$$\begin{aligned} \delta u = & -\frac{1}{2}\frac{\partial^2 v}{\partial x^2} - (n - b)v - p(Wu + Vv) \\ & - \text{Im}[f(x)] \int_{-\infty}^{\infty} 2G(x - \xi)\text{Im}[f(\xi)]v(\xi)d\xi \\ & - \text{Im}[f(x)] \int_{-\infty}^{\infty} 2G(x - \xi)\text{Re}[f(\xi)]u(\xi)d\xi. \end{aligned} \quad (8)$$

Here $G(x) = [1/(2d^{1/2})]\exp(-|x|/d^{1/2})$ is the response function of nonlocal nonlinearity. Above eigenvalue prob-

lem is solved numerically to find the maximum value of $Re(\delta)$. If $Re(\delta) > 0$, solitons are unstable. Otherwise, they are stable.

III. NONLOCAL DEFECT SOLITONS

In the PT-symmetric defective lattices with nonlocal nonlinearity, we find two types of defect solitons for positive, zero, and negative defects, respectively. The first type is the nodeless fundamental solitons, which can exist stably in the semi-infinite gap for all kinds of defects or in the first gap for negative defects. The other type of defect solitons, which exist in the first gap for all kinds of defects, is called dipole solitons in this paper, because most of them have two significant intensity peaks.

For positive defects, we assume $\epsilon = 0.5$ and the results are shown in Figs. 2 - 4. Figures 2(a) and 2(b) show that the power of soliton [defined as $P = \int_{-\infty}^{+\infty} |f(x)|^2 dx$] for both fundamental and dipole solitons increases almost linearly as increasing of propagation constant. As the nonlocality degree d increasing, the power of soliton increases too. The positive defect solitons vanish when the propagation constant is below the cutoff point, whose value does not depend on the nonlocality degree. This feature is similar to the case of traditional uniform lattices in nonlocal media [35].

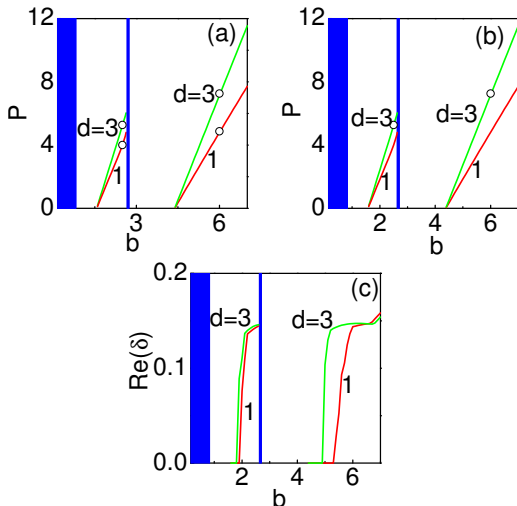


FIG. 2. (color online) Soliton power versus propagation constant for positive defect with (a) $W_0 = 0.1$ and (b) $W_0 = 0.15$. (c) The unstable growth rate $Re(\delta)$ for soliton solutions in (b). For all cases $\epsilon = 0.5$ and $p = 4$.

When $W_0 = 0.1$, the linear stability analysis shows that both fundamental and dipole solitons are stable in their whole regimes of existence in the semi-infinite gap and the first gap, respectively. For comparison, dipole solitons in the PT-symmetric defective lattices with local nonlinearity are stable only in a small region near the edge of the first gap [19]. It shows that the nonlocality expands the stability region of soliton. As W_0 increases,

the stability region of defect soliton decreases. Figure 2(c) shows the maximum growth rate $Re(\delta)$ for solitons with $W_0 = 0.15$. We can see that both fundamental and dipole solitons are unstable for the large propagation constant, and their stability regions become very narrow. We find that all fundamental solitons are unstable and their stability region disappears when $W_0 > 0.24$. For the dipole solitons in the first gap, the maximum value for existence of stable soliton is $W_0 = 0.16$.

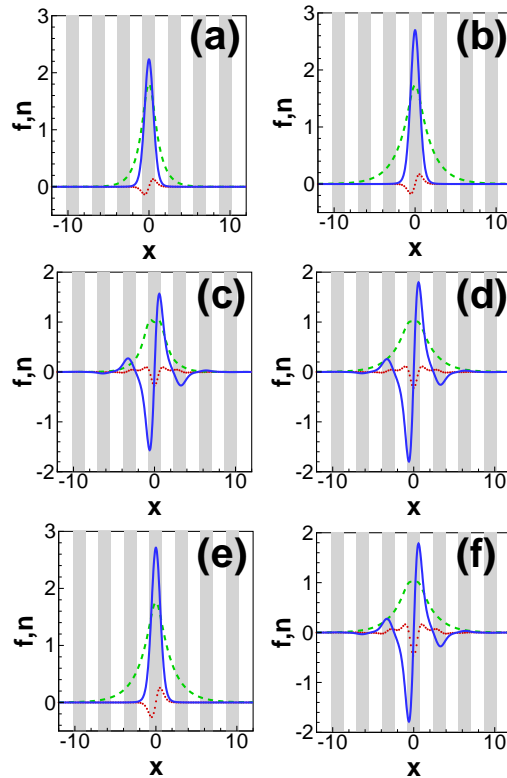


FIG. 3. (color online) The complex fields (solid blue: real part; dotted red: imaginary part) and the refractive-index changes (dashed green) for soliton solutions at (a) $b = 6$, $d = 1$; (b) $b = 6$, $d = 3$; (c) $b = 2.5$, $d = 1$; (d) $b = 2.5$, $d = 3$; (e) $b = 6$, $d = 1$; and (f) $b = 2.5$, $d = 3$; respectively. For all cases $\epsilon = 0.5$, $p = 4$. For (a)-(d) $W_0 = 0.1$ and (e)-(f) $W_0 = 0.15$.

The field profiles of the positive defect solitons are shown in Figs. 3(a)-3(f) for different W_0 and nonlocal degrees d , which correspond to the circle symbols in Figs. 2(a) and 2(b). Figures 3(a) and 3(b) show fundamental solitons in the semi-infinite gap for $W_0 = 0.1$, while dipole solitons in the first gap are shown in Figs. 3(c) and 3(d). One can see that the poles of dipole solitons are located inside the central channel of the lattice. As the nonlocality degree increases, the amplitudes of solitons increase but their shapes change very little. Figures 3(e) and 3(f) show the defect solitons for $W_0 = 0.15$. As the W_0 increases, the imaginary part of the field increases. The propagations corresponding to those solitons in Figs. 3(a)-3(f) are shown in Figs. 4(a)-4(f). The evolutions are

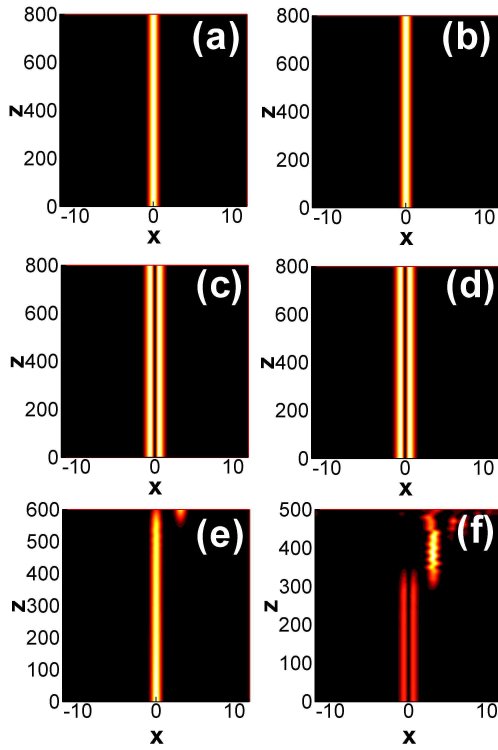


FIG. 4. (color online) (a)-(f) Evolutions of defect solitons corresponding to those in Figs. 3(a)- 3(f), respectively.

simulated based on Eqs. (1) and (4), and 1% random-noise perturbations are added into the initial input to verify the results of linear stability analysis. We can see that both fundamental solitons and dipole solitons are stable for $W_0 = 0.1$ but unstable for $W_0 = 0.15$.

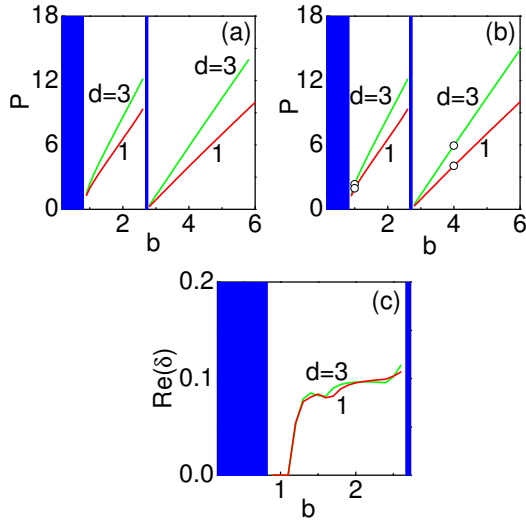


FIG. 5. (color online) Soliton power versus propagation constant for zero defect with (a) $W_0 = 0.05$ and (b) $W_0 = 0.1$, respectively. (c) The unstable growth rate $Re(\delta)$ for soliton solutions in (b). For all cases $\epsilon = 0$ and $p = 4$.

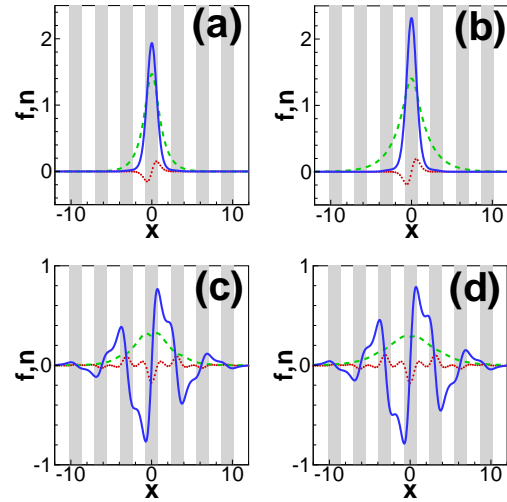


FIG. 6. (color online) The complex fields (solid blue: real part; dotted red: imaginary part) and the refractive-index changes (dashed green) for solitons in the semi-infinite gap at (a) $b = 4$, $d = 1$; (b) $b = 4$, $d = 3$; or solitons in the first gap at (c) $b = 1$, $d = 1$; and (d) $b = 1$, $d = 3$, respectively. For all cases $\epsilon = 0$, $p = 4$ and $W_0 = 0.1$.

Figures 5 and 6 show the results for zero defects ($\epsilon = 0$). The properties of defect solitons with zero defects are similar to those with positive defects. From Figs. 5(a) and 5(b), we can see that the cutoff points approach the lower edges of gaps. For $W_0 = 0.05$, fundamental solitons are stable in the whole semi-infinite gap, whereas dipole solitons are stable in the whole first gap. When $W_0 = 0.1$, dipole solitons are unstable for the large propagation constant, and their stability region becomes narrow, as shown in Fig. 5(c). The stability region of dipole solitons vanishes when $W_0 > 0.14$. Fundamental solitons are still stable in the whole semi-infinite gap for $W_0 = 0.1$, and their stability region begins to reduce when $W_0 > 0.12$. When $W_0 > 0.23$, all fundamental solitons become unstable. Figure 6 shows the complex profiles of solitons for zero defects, which correspond to the circle symbols in Fig. 5(b). Although the examples of solitons in the first gap [Figs. 6(c) and 6(d)] have more intensity peaks, the most of solitons in the first gap still have two significant peaks. The propagations of those examples for $W_0 = 0.1$ in Fig. 6 are all stable as the expectation by the linear stability analysis.

Next we study defect solitons in the nonlocal PT-symmetric lattices with negative defects, and results are shown in Figs. 7- 10. Fundamental solitons are found both in the semi-infinite gap [Fig. 7] and the first gap [Fig. 8], whereas dipole solitons exist in the first gap [Fig. 7]. It is interesting that there exists a maximum nonlocality degree d_{max} for some negative defect solitons. When the degree of nonlocal nonlinearity is above the maximum value, the fundamental solitons in the semi-infinite gap and the dipole solitons in the first gap do not exist. The maximum nonlocality degree depends

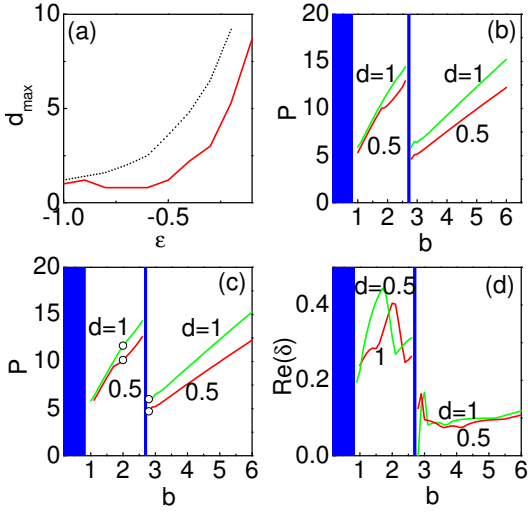


FIG. 7. (color online) (a) The maximum nonlocality degree d_{max} versus the depth of negative defect for fundamental solitons in the semi-infinite gap (dashed line) and dipole solitons in the first gap (solid red line). (b) and (c) Soliton power versus propagation constant for negative defects with (b) $W_0 = 0.05$ and (c) $W_0 = 0.1$, respectively. (d) The unstable growth rate $Re(\delta)$ for soliton solutions in (c). For all cases $p = 4$ and for (b)-(d) $\epsilon = -0.5$.

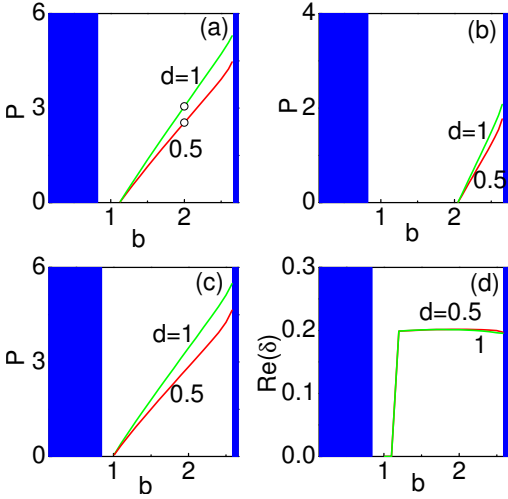


FIG. 8. (color online) Soliton power versus propagation constant for fundamental solitons in the first gap with (a) $W_0 = 0.1$, $\epsilon = -0.5$; (b) $W_0 = 0.1$, $\epsilon = -0.2$; and (c) $W_0 = 0.2$, $\epsilon = -0.5$, respectively. (d) The unstable growth rate $Re(\delta)$ for soliton solutions in (c). For all case $p = 4$.

on the depth of negative defects, as shown in Fig. 7(a). We can see that d_{max} decreases with increasing of the defect depth $|\epsilon|$. We also find similar phenomenon on the traditional defect solitons in non-PT-symmetric lattices with negative defects.

For negative defects, the linear stability analysis shows that fundamental solitons in the semi-infinite gap are stable in their whole existence region for $W_0 = 0.05$. As W_0

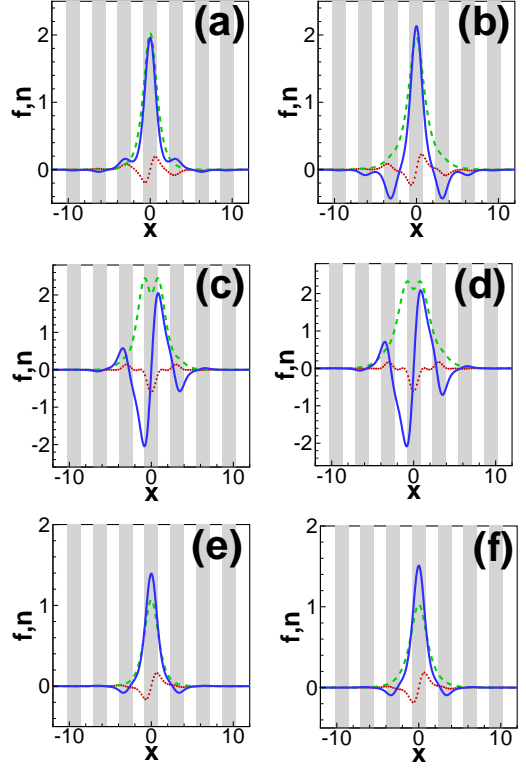


FIG. 9. (color online) The complex fields (solid blue: real part; dotted red: imaginary part) and refractive-index changes (dashed green) for soliton solutions in the semi-infinite gap at (a) $b = 2.8$, $d = 0.5$; (b) $b = 2.8$, $d = 1$; or soliton solutions in the first gap at (c) $b = 2$, $d = 0.5$; (d) $b = 2$, $d = 1$; (e) $b = 2$, $d = 0.5$; and (f) $b = 2$, $d = 1$, respectively. For all cases $\epsilon = -0.5$, $p = 4$ and $W_0 = 0.1$.

increases, the stability region reduces. For $W_0 = 0.1$, Fig. 7(c) shows that the fundamental solitons in the semi-infinite gap are unstable in the most existence region except at the edge of the gap when $d = 1$, whereas they are all unstable when $d = 0.5$. For comparison, the local defect solitons in the semi-infinite gap are unstable near the edge of the gap [19]. All fundamental solitons in the semi-infinite gap are unstable when $W_0 > 0.13$. The dipole solitons in the first gap are always unstable in the whole existence region for any value of W_0 .

Differing from the positive and zero defects, fundamental solitons can also exist stably in the first gap. Figures 8(a) - 8(c) show the power of fundamental solitons versus propagation constant in the first gap. We can see that there exists a cutoff point of propagation constant above which the fundamental solitons can exist. This feature is similar to the case of the positive and zero defects. The cutoff point shifts toward the low propagation constant with increasing of the depth of negative defect and the value of W_0 , and the existence region of fundamental solitons in the first gap increases too. When $W_0 = 0.1$, the fundamental solitons in the first gap are stable in their whole existence region, and their stability region begins

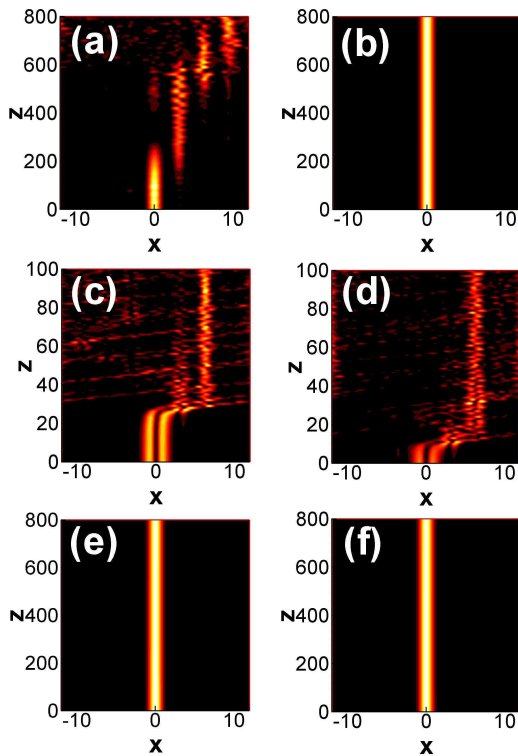


FIG. 10. (color online) (a)-(f) Evolutions of defect solitons corresponding to those in Figs. 9(a)- 9(f) respectively.

to reduce when $W_0 > 0.16$. When $W_0 = 0.2$, fundamental solitons is unstable in the most existence region except at the edge of the gap, as shown in Fig. 8(d). Their stability region vanishes when $W_0 > 0.23$.

The examples for the negative defect solitons are shown in Fig. 9, including the fundamental solitons in the semi-infinite gap [Figs. 9(a) and 9(b)], the dipole solitons in the first gap [Figs. 9(c) and 9(d)], and the fundamental solitons in the first gap [Figs. 9(e) and 9(f)], which correspond to the circle symbols in Fig. 7(c) and Fig. 8(a), respectively. Their corresponding propagations are shown in Figs. 10(a)-10(f). Figures 9(a) and 10(a) show the unstable fundamental soliton nearby the edge of the gap for $d = 0.5$, whereas, the fundamental soliton nearby the edge of the gap for $d = 1$ is stable as shown in Figs. 9(b) and 10(b). One can see that dipole solitons in the first gap are unstable [Figs. 10(c) and 10(d)], whereas fundamental solitons in the first gap are stable [Figs. 10(e) and 10(f)] for $W_0 = 0.1$.

In our study, all defect solitons are unstable for large W_0 when $p = 4$. However, the solitons in Ref. [4] is stable when $p = 1$ and $W_0 = 0.45$, which is close to the phase transition point ($W_0^c = 0.5$). So, we finally study the solitons with small modulation strength of the PT-symmetric potentials. We find that when the modulation depth of the PT-symmetric potentials is small, defect solitons can be stable for the positive defect and zero defect though W_0 is above the phase transition point. Figures 11(a)-11(c) show the examples of defect soli-

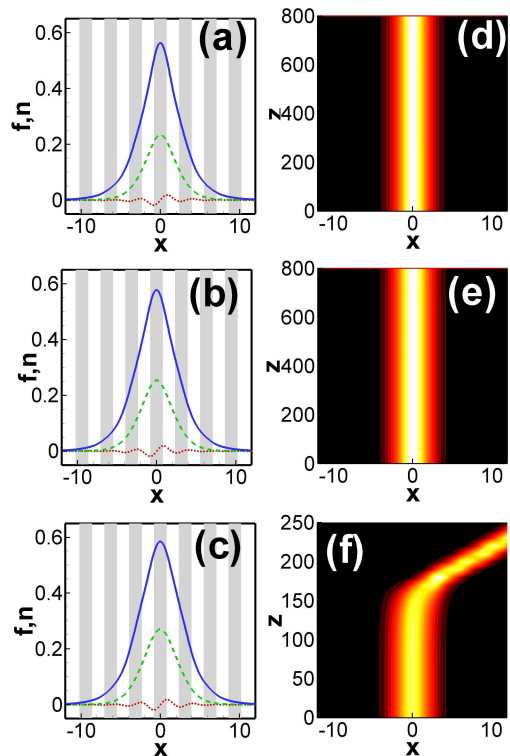


FIG. 11. (color online) The complex fields (solid blue: real part; dotted red: imaginary part) and the refractive-index changes (dashed green) of fundamental solitons with (a) positive defect $\epsilon = 0.5$, (b) zero defect $\epsilon = 0$, and (c) negative defect $\epsilon = -0.5$. (d)-(f) Evolutions of defect solitons corresponding to those in (a)-(c), respectively. For all cases $p = 0.1$, $W_0 = 0.55$, $b = 0.2$ and $d = 1$.

tons above the phase transition point, i.e. $p = 0.1$ and $W_0 = 0.55$, with positive defects ($\epsilon = 0.5$), zero defects ($\epsilon = 0$), and negative defects ($\epsilon = -0.5$), respectively. Figures 11(d)-11(f) show the corresponding propagations of those solitons. With the supporting of the nonlocal nonlinearity ($d = 1$), defect solitons with positive and zero defects are stable when W_0 is above the phase transition point, whereas they are unstable for negative defects. Here the self-guiding effect by the nonlocal nonlinearity plays more important role than the defect guiding effect, in balance with the diffraction and the transverse energy flowing induced by the imaginary part of Pt-symmetric lattice. In an other word, the nonlocal nonlinearity enhanced the real part of the PT potential, thus the nonlinearity can change the phase transition point equivalently [4].

IV. SUMMARY

In conclusion, we have studied the existence and stability of defect solitons supported by PT-symmetric nonlocal optical lattices. It is found that the nonlocality expands the stability region of defect solitons, especially

in the first gap. Fundamental solitons can exist stably in the semi-infinite gap for all kinds of defects or in the first gap for negative defects, whereas dipole solitons exist in the first gap for all kinds of defects. Most of defect solitons are stable for small value of W_0 , and their stability regions reduce and finally vanish as increasing W_0 . As an exception, dipole solitons with negative defects are always unstable for any value of W_0 . It is interesting that there exists a maximum nonlocality degree d_{max} for some negative defect solitons. We also find defect solitons with positive and zero defects can be stable even if the PT-symmetric potentials is above the phase transition point

when the modulation depth of the PT-symmetric lattices is small. These properties of the defect solitons in PT-symmetric nonlocal lattices are obviously different from those in the local PT-symmetric lattices. The various types of solitons may provide alternative methods in potential applications of synthetic PT-symmetric systems.

ACKNOWLEDGMENTS

This research was supported by the National Natural Science Foundation of China (Grant Nos. 10804033, 11174090 and 11174091).

-
- [1] C. M. Bender, D. C. Brody, and H. F. Jones, *J. Math. Phys.* **40**, 2201 (1999).
 - [2] C. M. Bender, D. C. Brody, and H. F. Jones, *Am. J. Phys.* **71**, 1095 (2003).
 - [3] R. El-Ganainy, K. G. Makris, D. N. Christodoulides, and Ziad H. Musslimani *Opt. Lett.* **32**, 2632 (2007).
 - [4] Z. H. Musslimani, K. G. Makris, R. El-Ganainy, and D. N. Christodoulides, *Phys. Rev. Lett.* **100**, 030402 (2008).
 - [5] K. G. Makris, R. El-Ganainy, D. N. Christodoulides, and Z. H. Musslimani, *Phys. Rev. Lett.* **100**, 103904 (2008).
 - [6] C. T. West, T. Kottos, and T. Prosen, *Phys. Rev. Lett.* **104**, 054102 (2010).
 - [7] O. Bendix, R. Fleischmann, T. Kottos, and B. Shapiro, *Phys. Rev. Lett.* **103**, 030402 (2009).
 - [8] A. E. Miroshnichenko, B. A. Malomed, and Y. S. Kivshar, *Phys. Rev. A* **84**, 012123 (2011).
 - [9] A. Guo, G. J. Salamo, D. Duchesne, R. Morandotti, M. Volatier-Ravat, V. Aimez, G. A. Siviloglou, and D. N. Christodoulides, *Phys. Rev. Lett.* **103**, 093902 (2009).
 - [10] C. E. Ruter, K. G. Makris, R. El-Ganainy, D. N. Christodoulides, M. Segev, and D. Kip *Nature Phys.* **6**, 192 (2010).
 - [11] M. C. Zheng, D. N. Christodoulides, R. Fleischmann, and T. Kottos, *Phys. Rev. A* **82**, 010103 (2010).
 - [12] H. Ramezani, T. Kottos, R. El-Ganainy, and D. N. Christodoulides, *Phys. Rev. A* **82**, 043803 (2010).
 - [13] A. A. Sukhorukov, Z. Y. Xu, and Y. S. Kivshar, *Phys. Rev. A* **82**, 043818 (2010).
 - [14] Z. Lin, H. Ramezani, T. Eichelkraut, T. Kottos, H. Cao, and D. N. Christodoulides, *Phys. Rev. Lett.* **106**, 213901 (2011).
 - [15] F.Kh. Abdullaev, Y. V. Kartashov, V.V. Konotop, and D. Zezyulin, *Phys. Rev. A* **83**, 043805(R) (2011).
 - [16] D. A. Zezyulin, Y. V. Kartashov, and V.V. Konotop, *Europhysics Letters* **96**, 64003 (2011).
 - [17] X. Zhu, H. Wang, L. X. Zheng, H. G. Li, and Y. J. He, *Opt. Lett.* **36**, 2680 (2011).
 - [18] K. Y. Zhou, Z. Y. Guo, J. C. Wang and S. T. Liu, *Opt. Lett.* **35**, 2928 (2010).
 - [19] H. Wang and J. Wang, *Opt. Express* **19**, 4030 (2011).
 - [20] Z. E. Lu, and Z. M. Zhang *Opt. Express* **19**, 11457 (2011).
 - [21] F. Ye, Y. V. Kartashov, V. A. Vysloukh, and L. Torner, *Phys. Rev. A* **78**, 013847 (2008).
 - [22] Y. Li, W. Pang, Y. Chen, Z. Yu, J. Zhou, and H. Zhang, *Phys. Rev. A* **80**, 043824 (2009).
 - [23] V. A. Brazhnyi, V. V. Konotop, and V. M. Perez-Garcia, *Phys. Rev. Lett.* **96**, 060403 (2006).
 - [24] F. Fedele, J. Yang, and Z. Chen, *Opt. Lett.* **30**, 1506 (2005).
 - [25] D. K. Campbell, S. Flach, and Y. S. Kivshar, *Phys. Today* **57**, 43 (2004).
 - [26] M. Segev, B. Crosignani, A. Yariv, and B. Fischer, *Phys. Rev. Lett.* **68**(7), 923 (1992).
 - [27] M. Segev, G. C. Valley, B. Crosignani, P. DiPorto, and A. Yariv, *Phys. Rev. Lett.* **73**(24), 3211 (1994).
 - [28] W. Krolikowski, M. Saffman, B. Luther-Davies, and C. Denz, *Phys. Rev. Lett.* **80**(15), 3240 (1998).
 - [29] C. Conti, M. Peccianti, and G. Assanto, *Phys. Rev. Lett.* **91**, 073901 (2003).
 - [30] C. Conti, M. Peccianti, and G. Assanto, *Phys. Rev. Lett.* **92**, 113902 (2004).
 - [31] M. Peccianti, K. A. Brzdakiewicz, and G. Assanto, *Opt. Lett.* **27**, 1460 (2002).
 - [32] C. Rotschild, O. Cohen, O. Manela, M. Segev, and T. Carmon *Phys. Rev. Lett.* **95**, 213904 (2005).
 - [33] B. Alfassi, C. Rotschild, O. Manela, M. Segev, and D. N. Christodoulides, *Phys. Rev. Lett.* **98**, 213901 (2007).
 - [34] A.W. Snyder and D. J. Mitchell, *Science* **276**, 1538 (1997).
 - [35] Z. Xu, Y. V. Kartashov, and L. Torner, *Phys. Rev. Lett.* **95**, 113901 (2005).
 - [36] D. Buccoliero, A. S. Desyatnikov, W. Krolikowski, and Y. S. Kivshar, *Phys. Rev. Lett.* **98**, 053901 (2007).
 - [37] N. Ghofraniha, C. Conti, G. Ruocco and S. Trillo, *Phys. Rev. Lett.* **99**, 043903 (2007).
 - [38] C. Conti, A. Fratallocchi, M. Peccianti, G. Ruocco, and S. Trillo, *Phys. Rev. Lett.* **102**, 083902 (2009).
 - [39] W. Hu, T. Zhang, Q. Guo, X. Li, and S. Lan, *Appl. Phys. Lett.* **89**, 071111 (2006).
 - [40] N. I. Nikolov, D. Neshev, O. Bang, and W. Z. Krolikowski, *Phys. Rev. E* **68**, 036614 (2003).
 - [41] P. V. Larsen, M. P. Sorensen, O. Bang, W. Z. Krolikowski, and S. Trillo, *Phys. Rev. E* **73**, 036614 (2006).
 - [42] R. Bekenstein and M. Segev, *Opt. Express* **19**, 23706-23715(2011).
 - [43] J. Yang, and T. I. Lakoba, *Stud. Appl. Math.* **118**, 153-197 (2007).